Langmuir

Letter

pubs.acs.org/Langmuir

Direct Visualization of Bactericidal Action of Cationic Conjugated Polyelectrolytes and Oligomers

Ying Wang,[†,‡] Thomas S. Corbitt,[†] Stephen D. Jett,[§] Yanli Tang,[∥] Kirk S. Schanze,[⊥] Eva Y. Chi,[†] and David G. Whitten*[,†]

[†]Department of Chemical and Nuclear Engineering, Center for Biomedical Engineering, [‡]Department of Chemistry and Chemical Biology, and [§]Department of Cell Biology and Physiology, University of New Mexico, Albuquerque, New Mexico 87131-1341, United States

[∥]School of Chemistry and Chemical Engineering, Shaanxi Normal University, Xi'an, Shaanxi 710062, China

[⊥]Department of Chemistry, University of Florida, Gainesville, Florida 32611-7200, United States

ABSTRACT: The bactericidal mechanisms of poly(phenylene ethynylene) (PPE)-based cationic conjugated polyelectrolytes (CPE) and oligophenylene ethynylenes (OPE) were investigated using electron/optical microscopy and small-angle X-ray scattering (SAXS). The ultrastructural analysis shows that polymeric PPE-Th can significantly remodel the bacterial outer membrane and/or the peptidoglycan layer, followed by the possible collapse of the bacterial cytoplasm membrane. In contrast, oligomeric end-only OPE (EO-OPE) possesses potent bacteriolysis activity, which efficiently disintegrates the bacterial cytoplasm membrane and induces the release of bacterial cell content. Using single giant vesicles and SAXS, we demonstrated that the membrane perturbation mechanism of EO-OPE against model bacterial membranes results from a 3D membrane phase transition or perturbation.

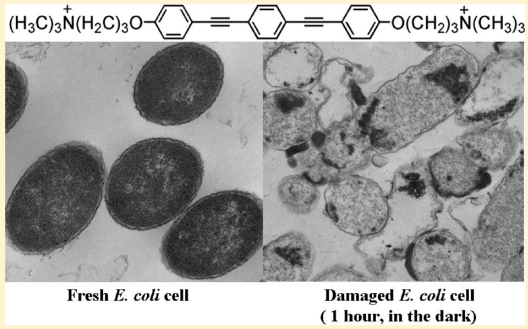

INTRODUCTION

The outbreak of global infectious diseases has provoked an urgent need to discover novel antimicrobial agents.[1,2] As a result, naturally occurring antimicrobial peptides and synthetic polymers have been widely studied as potential antimicrobial agents for combating pathogens in bulk solutions or immobilized on surfaces.[3−6] Recently, a series of poly(*p*-phenylene ethynylene) (PPE)-based conjugated polyelectrolytes (CPEs) and oligo(*p*-phenylene ethynylene)s (OPEs) with controlled chain lengths and functional groups have attracted significant interest because of their ability to kill bacteria and viruses[7−10] and their applications to biosensing.[11,12] In general, these CPE and OPE compounds exhibit broad spectrum and rapid light-activated biocidal activities and moderate killing efficiencies in the dark.[13] Furthermore, both the light-activated and dark biocidal activities of CPEs and OPEs are believed to be initiated by their interactions with the bacterial outer envelopes. Therefore, the main focus of the current study is to understand the lethal effect of the CPEs and OPEs against bacteria in the dark, which is also a part of our structure−activity relationship study.

The biocidal activity and selectivity of the CPE, OPE, and other antimicrobial compounds can be related to their membrane perturbation ability.[14−18] However, for some of the biocidal materials, their antimicrobial activity may also stem from the interaction with other bacterial outer envelope components, such as membrane-embedded proteins and lipopolysaccharides (LPS).[5,19,20] In other words, their membrane activity may only partially account for the antimicrobial ability. Although some insights have been gained about CPE's and OPE's biocidal and membrane activities,[21] little is known about their mechanism or mode of binding to the bacterial outer envelope or the subsequent key toxicity-inducing events.

There are significant structural differences between the outer envelopes of gram-negative and gram-positive microorganisms. The outer envelope of gram-negative bacteria is composed of an outer membrane and a cytoplasm membrane (or inner membrane) that are separated by a thin, intermittently cross-linked peptidoglycan network. The outer leaflet of the gram-negative bacterial outer membrane contains high levels of LPS. However, gram-positive bacteria only have one lipid membrane (cytoplasm membrane) covered by a thick layer of heavily cross-linked peptidoglycan.[22] In both cases, the peptidoglycan layer does not provide an efficient barrier against the diffusion of small solutes.[23] Moreover, protein is another essential component of both gram-negative and gram-positive bacterial outer envelopes. Generally, gram-negative bacteria exhibit higher resistance to antimicrobial agents than do gram-positive microorganisms, which is due to the more complicated outer envelope structure of the gram-negative bacteria.[24] Specifically, the presence of the porin channels on the outer membrane of gram-negative bacteria significantly impairs the penetration

Received: November 12, 2011
Revised: December 5, 2011
Published: December 7, 2011

Scheme 1. Structures of the Antimicrobial Compounds Used in This Study, Where *N* Denotes the Number of Repeat Units

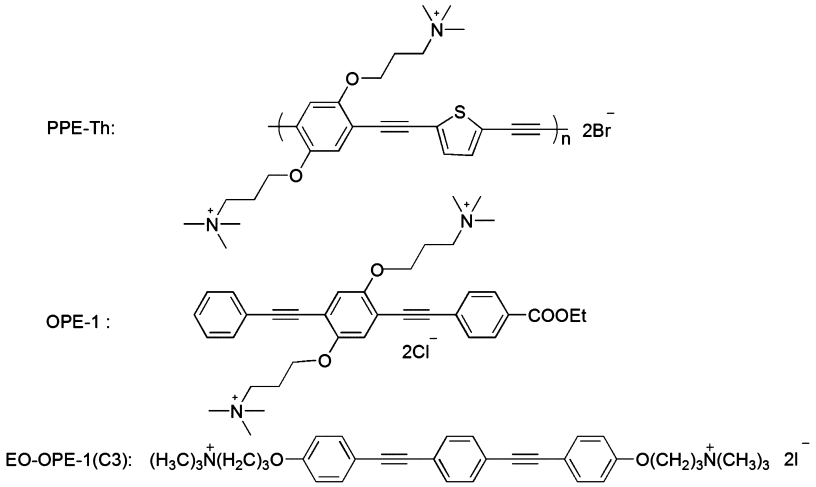

ability of antimicrobial agents into the cell.[23] One important common characteristic of both gram-negative and gram-positive bacterial cell envelopes is the net negative charge, which is provided by LPS for gram-negative bacteria, teichoic acids for gram-positive bacteria, and the anionic phospholipids from the bacterial cytoplasm membrane and/or the outer membrane, such as phosphatidylglycerol (PG) and cardiolipin (CL).[25] For gram-negative bacteria, the negatively charged outer membrane serves as the first point of contact for the cationic antimicrobial compounds. Furthermore, the amphiphilic nature of the CPEs and OPEs may enhance their ability to denature membrane proteins and perturb lipid membranes via hydrophobic interactions. As a result, the bacterial outer envelope should be one of the main sites of attack for the CPEs and OPEs because of the favorable electrostatic and hydrophobic interactions.

Three PPE-based cationic compounds with different structures, which exhibited various toxicity against *Escherichia coli* (*E. coli*),[19] were chosen for this study to explore the structure–antimicrobial activity relationship (Scheme 1).[9,26,27] Because of large differences in molecular weight and the spatial arrangement of the positively charged side and end groups, the interactions of these antimicrobial compounds with the bacterial outer envelope were expected to be different, and it was anticipated that these differences could result in different mechanisms of action against gram-negative bacteria. In this study, we examined the toxicity mechanisms of the three antimicrobial compounds. In particular, the direct visualization of damage to the bacterial outer envelope and changes to the bacterial morphology were found via scanning and transmission electron microscopy (SEM and TEM) imaging of *E. coli* cells exposed to the three compounds. The imaging of single giant vesicles and small-angle X-ray scattering (SAXS) measurements of unilamellar vesicles provide further insights into the membrane perturbation mechanisms for the oligomeric OPEs used in this study. Laser scanning confocal microscopy (LSCM) gives additional detailed information on the antimicrobial mechanism of OPE-1.

EXPERIMENTAL METHODS

Materials. The antimicrobial compounds (Scheme 1) used in this study were synthesized as reported.[9,26,27] Lipids[28] and lipid vesicle extrusion supplies were purchased from Avanti Polar Lipids (Alabaster, AL) and used as received. All other chemicals were purchased from Sigma-Aldrich (St. Louis, MO) or BD Biosciences (Franklin Lakes, NJ). *E. coli* strains ATCC 11303 and ATCC 29425 were obtained from the American Type Culture Collection (ATCC, Manassas, VA). *P. aeruginosa* strain PAO1 was a generous gift from Dr. Tim Tolker-Nielsen. Ultrapure water was used throughout the study (Milli-Q, 18.2 MΩ cm^{-1} resistivity).

Electron and Optical Microscopy. Fresh *E. coli* (ATCC 11303) cells in the exponential growth phase (~10^8 colony-forming units (CFU)/mL)) were incubated with 10 μg/mL PPE-Th, OPE-1, or EO-OPE-1(C3) in the dark for 1 h and imaged by SEM as previously described.[19] For TEM imaging, cell pellets were fixed with 2% glutaraldehyde for 1 day and then 1% osmium tetroxide for 1 hour at room temperature. The samples were dehydrated by sequential treatment with increasing concentrations of ethanol. Then, the cells were embedded in resin (Spurr's resin kit, Electron Microscopy Sciences, Hatfield, PA), sectioned, and imaged by TEM (Hitachi H7500, Tokyo, Japan). *E. coli* (ATCC 29425) and PAO1 cells (~10^8/mL) were incubated with OPE-1 (42.5 μg/mL) for 60 min in 0.85% NaCl sterile solution and kept in the dark. Then, the samples were stained with SYTO 60/SYTOX Green[29] (Molecular Probes, Carlsbad, CA) and examined by laser scanning confocal microscopy (Zeiss LSM 510 Meta, Thornwood, NY) as described previously.[30]

Formation and Observation of Giant Vesicles. Giant vesicles were prepared and observed by a method modified from the literature.[31,32] Lipid mixtures (*E. coli* total lipids extract, DMPE-Rh, and Biotin-PEG-DSPE in a molar ratio of 97:0.5:2.5, respectively) were dissolved in chloroform, dried, and rehydrated with 10 mM 2-[4-(2-hydroxyethyl)-1-piperazinyl]ethanesulfonic acid (HEPES, pH 7.4) to a final concentration of 0.33 mg/mL at 37 °C for 2 h. The observation microchambers (internal volume ~100 μL) were made from microscope slides and coverslips and sealed with double-sided tape. The microchamber was incubated with neutravidin solution (0.1 mg/mL in 10 mM HEPES) for 15 min. After being rinsed with the HEPES buffer, the microchamber was incubated with the giant vesicle solution for 5 min and then rinsed again to remove unattached vesicles. A 2 μL aliquot of oligomeric OPEs (50 μg/mL in 10 mM HEPES) was added to the chamber. The immobilized vesicles were then imaged with a fluorescence microscope (Zeiss Imager A2, BP 545/25 nm excitation filter, BP 605/70 nm emission filter, Thornwood, NY).

X-ray Scattering. SAXS experiments were carried out at the Stanford Synchrotron Radiation Laboratory (Palo Alto, CA) (BL4-2) as described in the literature.[33] Briefly, the *E. coli* total lipid extract or mixed 8:2 (molar ratio) DOPE/DOPG lipids were dissolved in chloroform, dried, and rehydrated with Millipore water to a final concentration of 25 mg/mL at room temperature. The vesicle solutions were sonicated and extruded through a 100 nm polycarbonate membrane (Avanti) to make small unilamellar vesicles (SUV). EO-OPE-1(C3) (7.6 mg/mL) was prepared in 10% DMSO in

dx.doi.org/10.1021/la2044569 | *Langmuir* 2012, 28, 65–70

water and mixed with SUVs at various OPE-to-lipid molar ratios. SAXS data were collected using 11 keV X-rays.

RESULTS AND DISCUSSION

Many naturally occurring and synthetic antimicrobial agents with cationic and amphiphilic properties exert their toxicity by disrupting the integrity of bacterial cells.[5,34,35] Moreover, small hydrophilic molecules are readily able to penetrate the bacterial outer membrane and/or peptidoglycan layer.[35] Therefore, CPEs and OPEs with different molecular weights may penetrate the bacterial outer envelope to various extents, leading to different toxic mechanisms of action.

PPE-Th and EO-OPE-1(C3) Antimicrobial Activity Visualized by SEM and TEM. SEM and TEM were used to image the structural changes on *E. coli* cells upon incubation with the antimicrobial agents. As shown in Figure 1 (A1, B1, and C1), the *E. coli* cells alone maintain their integrity with a smooth cell surface and the intact bacterial outer envelopes are clearly seen. After 1 h of incubation in the dark, the *E. coli* cells (10^8 CFU/mL) exposed to PPE-Th or EO-OPE-1(C3) (10 μg/mL) show striking but different structural damage. The surfaces of PPE-Th-treated cells appear to be rougher (Figure 1A2), and the cell outer membrane is significantly remodeled by the polymer, possibly leading to the formation of blebs on the bacteria surface (arrows in Figure 1B2,C2). In addition, an obvious but small population of PPE-Th treated cells is empty (arrow in Figure 1D2), which implies that these cells have released their content as a result of their compromised cell integrity. A remarkable characteristic of the EO-OPE-1(C3)-treated cells is the appearance of abundant amorphous material, presumably cell content (Figure 1A3). TEM images confirm the collapse of bacterial structure induced by EO-OPE-1(C3) in which a large number of empty or partially empty cells with debris are observed (Figure 1B3,C3). Moreover, TEM imaging also captured the site and processing of the release of internal cell content from some bacteria (arrow in Figure 1D3).

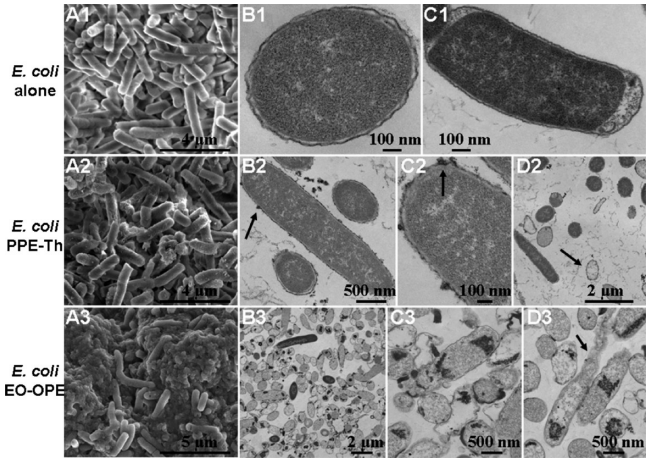

Figure 1. SEM (A1, A2, and A3) and TEM (B1-D3) micrographs of *E. coli* (ATCC 11303) cells (10^8 CFU/mL) alone (A1, B1, and C1) and incubated with 10 μg/mL PPE-Th (A2, B2, C2, and D2) and EO-OPE-1(C3) (A3, B3, C3, and D3) for 1 h in the dark. Panel A1 is reprinted with permission from ref 19.

It has been previously observed that the addition of polymeric PPE-Th can cause *E. coli* cells to aggregate and precipitate.[19] In contrast, EO-OPE-1(C3) was found to decrease the optical density of a *E. coli* cell suspension and induce the release of 260 nm absorbing materials (e.g., DNA and protein), which may be caused by the lysis of the cells.[19] PPE-Th and EO-OPE-1(C3) represent two extremes in our current antimicrobial agent library. Polymeric PPE-Th is large and fairly hydrophobic and tends to form large aggregates in aqueous solution.[30] However, EO-OPE-1(C3) with functional cationic groups on the molecular termini is a small, needlelike molecule. Jérôme et al. proposed that antimicrobial polycationic compounds with relatively high molecular weights may exert toxicity against gram-negative bacteria via binding strongly to LPS, leading to the disruption of the cell outer membrane.[5] Because of the attractive electrostatic and/or hydrophobic interactions, PPE-Th may bind strongly to the bacterial outer membrane, but its ability to penetrate the outer membrane and peptidoglycan layer may be limited by its large molecular size. As a result, polymeric PPE-Th binds to a bacterial surface and causes damage predominately to the surface of bacteria, including the induction of cell agglomeration; after that, PPE-Th may also further damage the bacterial cytoplasm membrane and induce cell content release. However, the small, needlelike features of EO-OPE-1(C3) may provide the oligomer the ability to permeate the outer membrane and the peptidoglycan layer and allow it to disrupt the cytoplasm membrane, leading to the lysis of the bacteria. Taken together, a general bactericidal action scheme for the polymeric CPEs and oligoermic OPEs is proposed in Figure 2,[19] and it is reasonable to apply this model to other antimicrobial agents with similar structures.

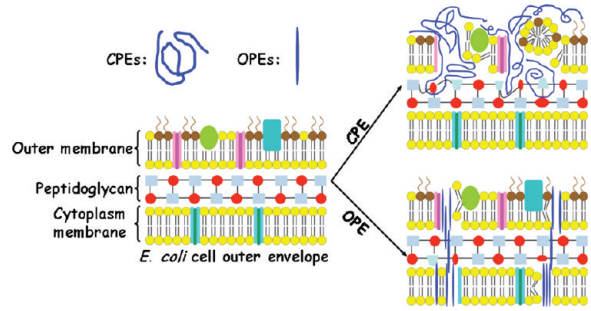

Figure 2. Proposed antimicrobial mechanism for CPEs and OPEs in the dark. Reprinted and modified with permission from ref 19.

Effect of OPE-1 on Gram-Negative Bacteria. OPE-1 and EO-OPE-1(C3) share the same molecular backbone and are of similar sizes but have different spatial arrangements of the cationic functional groups (Scheme 1), which may result in different antimicrobial activities[8,9,19] and mechanisms of action. Generally, OPE-1's dark biocidal activity is not as great as that of other CPEs or OPEs.[8,19] Herein, the lethal effect of OPE-1 on two gram-negative bacteria is examined by LSCM imaging, which is capable of tracking real-time changes to the structure of bacteria. As shown in Figure 3A1,A2, most of the untreated bacteria were live. However, a significant number of bacteria were killed and agglomerated by the addition of OPE-1 under specific experimental conditions (Figure 3B1,B2). Interestingly, the release of fibrous and threadlike materials, probably cell content, from dead bacteria is clearly observed (arrows in Figure 3D1,D2). As described earlier,[19] OPE-1 can induce membrane depolarization in *E. coli*, which implies that the cell transmembrane electrochemical gradient is perturbed by OPE-1.[19,36] As a result, the microorganisms may not be able to

dx.doi.org/10.1021/la2044569 | *Langmuir* 2012, 28, 65–70

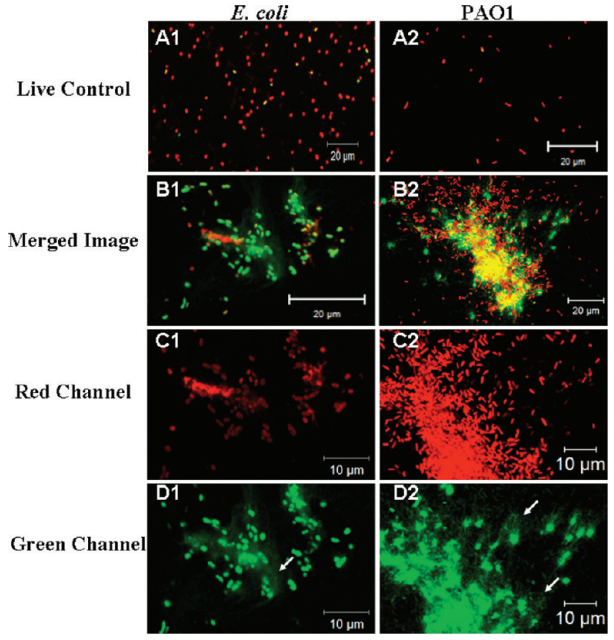

Figure 3. LSCM imaging of *E. coli* (ATCC 29425) and PAO1 cells (~10^8/mL) alone (A1 and A2) and treated with 42.5 μg/mL OPE-1 (B1 and B2) in the dark. The merged images are further split into a red channel (C1 and C2, live bacteria) and a green channel (D1 and D2, dead bacteria).

generate energy and the water and ion flow across the membrane may become disregulated, leading to possible cell swelling and/or lysis.[37] Moreover, for both *E. coli* and PAO1, some of the dead bacteria (Figure 3D1,D2) seem to be larger than the corresponding live bacteria (Figure 3C1,C2), which may result from a single swelling dead bacterium and/or the aggregation of dead bacteria. TEM imaging also confirms the loss of cell content from *E. coli* induced by OPE-1 (Figure 4).

Membrane Perturbation Actions of OPE-1 and EO-OPE-1(C3). All of the studies described above point to the different mechanisms of action for polymeric PPE-Th and oligomeric OPEs. Steric hindrance due to the high molecular weight of PPE-Th may prevent the polymer from penetrating the outer membrane and the peptidoglycan layer from reaching the cytoplasm membrane. In contrast, small, rodlike EO-OPE-1(C3) exhibits remarkable bacteriolysis activity, which is related to its membrane perturbation activity. In addition, the low molecular weight and side functional groups of OPE-1 may also provide the oligomer the ability to penetrate the bacterial outer membrane and interact with the cytoplasm membrane. However, its membrane perturbation and dark antimicrobial abilities are less than that of EO-OPE-1(C3).[8,9,14]

The membrane perturbation actions of OPE-1 and EO-OPE-1(C3) were visualized and compared by imaging single giant vesicles. Upon the addition of OPE-1 to giant vesicles composed of *E. coli* total lipids, the vesicle disintegrated and disappeared quickly. Thus, OPE-1 is efficiently incorporated into the lipid bilayer and may induce lipid phase separation followed by the lysis of the vesicle structure (Figure 5A), which

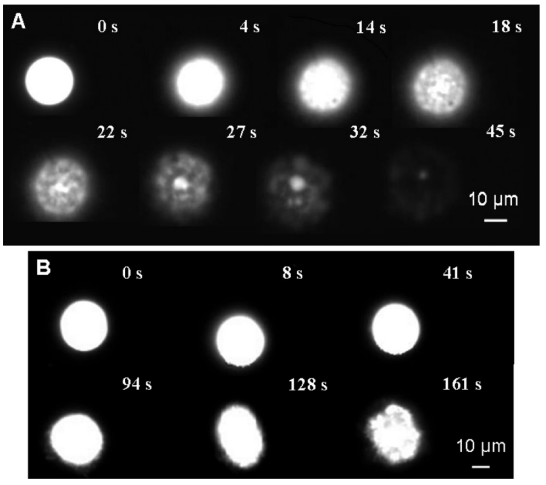

Figure 5. Time lapse fluorescence microscopy images showing the damage to a giant vesicle caused by the addition of OPE-1 (A) and EO-OPE-1(C3) (B) at room temperature. The vesicle is composed of the *E. coli* total lipid and labeled with DMPE-Rh and Biotin-PEG-DSPE (0.5 and 2.5 mol %, respectively). The elapsed time after the addition of the antimicrobial agent is labeled for each image.

may follow the carpet or detergent-like membrane-destabilizing model.[38] EO-OPE-1(C3) can also dramatically change the morphology of the lipid vesicle. However, the residual lipid-OPE structure was still observable, and no further morphology changes or vesicle disintegration occurred even upon prolonged observation (image not shown). It is worth noting that as a control the addition of 10 mM HEPES buffer alone did not cause any visible damage to the vesicle (data not shown). Quantitatively, EO-OPE-1(C3) possesses a much higher membrane perturbation ability against both model bacterial and mammalian cell membranes than OPE-1.[14] Herein, the single giant vesicle assay is employed as a qualitative measurement to observe the membrane disruption actions for the OPEs used for the current study. The actual concentration of the OPEs interacting with the vesicle is difficult to determine but is estimated to be much lower than 50 μg/mL (Experimental Methods).

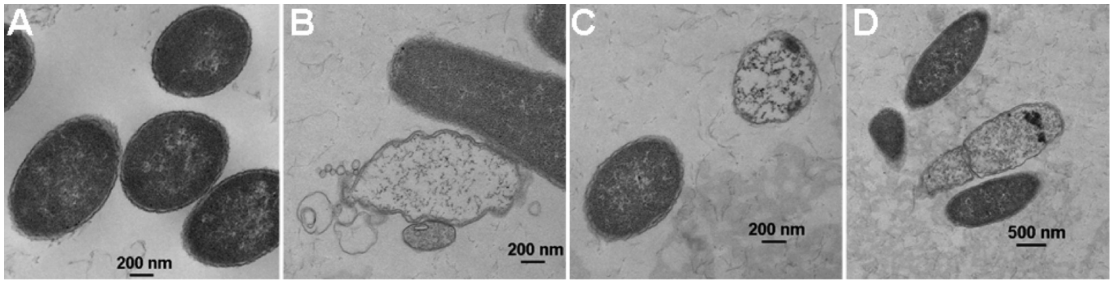

Figure 4. TEM micrographs of *E. coli* cells alone (A) and incubated with 10 μg/mL OPE-1 (B–D) for 1 h in the dark.

dx.doi.org/10.1021/la2044569 | *Langmuir* 2012, 28, 65–70

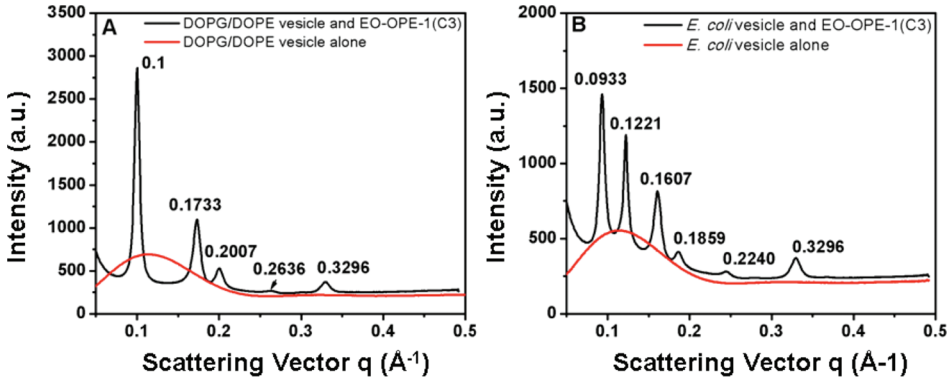

Figure 6. SAXS data for EO-OPE-1(C3) (3.8 mg/mL) complexed with 20:80 DOPG/DOPE (12.5 mg/mL) (A) and *E. coli* total lipid (12.5 mg/mL) (B) model membranes.

As described above, the potent antimicrobial activity of EO-OPE-1(C3) stems from its high membrane activity; it is of particular interest to investigate its membrane perturbation mechanism by SAXS further. In addition to vesicles composed of the *E. coli* total lipid extract, vesicles made of 20:80 DOPG/DOPE were also used for the SAXS assay (Experimental Methods).[15,33] For vesicles alone, only one broad peak with low scattering intensity is detected for each lipid composition (Figure 6, red lines), which suggests the existence of a lamellar phase for the SUVs.[33] After exposure to EO-OPE-1(C3), scattering profiles of the vesicles dramatically changed. Multiple new, sharp scattering peaks are observed in both membrane systems. The peak at q = 0.3296 Å^{-1} is due to EO-OPE-1(C3) (data not shown). The peak positions (q values) of the DOPG/DOPE model membrane exposed to EO-OPE-1 have a characteristic ratio of 1:$(3)^{1/2}$:2:$(7)^{1/2}$, indicative of an inverted hexagonal phase (Figure 6A).[39] A similar trend is observed for the vesicles composed of the more complex *E. coli* total lipids (Figure 6B), although the exact positions of the new peaks deviate from that of an inverted hexagonal phase and the nature of the new lipid phase at present is unclear. Tew and co-workers have systematically investigated the membrane perturbation activity of a series of antimicrobial *m*-phenylene ethynylene oligomers via SAXS and other technologies.[15,40] Similar to what we have observed for EO-OPE-1(C3), one of Tew's membrane active oligomers, AMO-2, was capable of forming a complex with *E. coli* lipid membranes/vesicles and inducing a hexagonal structure. The deviation of the SAXS peak positions from the characteristic inverted hexagonal phase has been attributed to the complex lipid distribution from the bacterial membrane extracts.[15] As described in the single giant vesicle imaging section, the EO-OPE-1(C3) and *E. coli* membrane complex was not soluble in the aqueous solvent, which also supports the assumption of the possible formation of a hydrophobic inverted hexagonal complex (Figures 5B and 6B). At the current stage, we cannot rule out the possibility of the formation of other bicontinuous cubic phases[41] for the EO-OPE-1(C3) and *E. coli* membrane complex. However, these changes indicate that the oligomer is capable of inducing specific structural changes in the lamellar lipid phase. Wimley proposed the interfacial activity model to explain the membrane activity of antimicrobial peptides.[42] On the basis of Wimley's theory and our previous dye release assays,[14] OPE-1 and EO-OPE-1(C3) may not be able to induce the formation of permanent transmembrane pores in lipid vesicles such as barrel stave pores. Results from this study, combined with our previous work,[38] indicate that the OPEs first attach to the negatively charged membrane surfaces and then induce membrane collapse and/or phase transitions via a carpet or detergent-like mechanism. Although OPE-1 and PPE-Th possess intrinsic low or compromised membrane perturbation activity against bacteria, these compounds may interact with the bacterial cytoplasm membrane to certain extents. Therefore, further characterizations of the membrane perturbation mechanism of PPE-Th and OPE-1 via SAXS are now underway.

CONCLUSIONS

The current study presents the interactions of cationic CPE and OPE compounds with the bacterial outer envelope and model bacterial membrane. Our results indicate that (1) cationic PPE-Th with a high molecular weight has a high affinity for the negatively charged bacterial outer membrane components and can kill the bacteria via destabilizing the bacterial outer membrane and/or the peptidoglycan layer and (2) small oligomeric OPEs can exert toxicity against bacteria primarily by inducing cytoplasm membrane collapse and/or perturbing the cell's transmembrane electrochemical gradient. In addition, the fact that the biocidal pathways of the CPE and OPE compounds operate by physically compromising the bacterial integrity make it difficult for the bacteria to develop resistance, making this class of compounds promising candidates to address the global problem of multidrug antibiotic resistance.

AUTHOR INFORMATION

Corresponding Author

*E-mail: whitten@unm.edu..

Author Contributions

Y.W. performed the SEM imaging and giant vesicle and SAXS work. Y.T. performed LSCM imaging and synthesized OPE-1. T.S.C. provided assistance on LSCM imaging. S.D.J. carried out the TEM imaging. E.Y.C., K.S.S., and D.G.W. provided guidance and advice. This letter was written through the contributions of all authors, and all authors have given approval to the final version of the letter.

ACKNOWLEDGMENTS

This research is financially supported by the Defense Threat Reduction Agency (contract no. W911NF07-1-0079). We gratefully acknowledge help from Dr. Zhijun Zhou of the Center for Biomedical Engineering at the University of New Mexico for providing the antimicrobial agents. We thank the Stanford Synchrotron Radiation Laboratory for providing

access to the SAXS facility and Dr. Tsutomu Matsui for assistance with SAXS data collection. TEM data were generated in the UNM Electron Microscopy Shared Facility supported by the University of New Mexico Health Sciences Center and the University of New Mexico Cancer Center. Y.W. also thanks the University of New Mexico for the Research Project and Travel (RPT) Grants.

REFERENCES

(1) Moellering, R. C. Jr. *N. Engl. J. Med.* **2010**, *363*, 2377−2379.
(2) Moellering, R. C. Jr. *Int. J. Antimicrob. Agents* **2011**, *37*, 2−9.
(3) Brogden, K. A. *Nat. Rev. Microbiol.* **2005**, *3*, 238−250.
(4) Kenawy, E. R.; Worley, S. D.; Broughton, R. *Biomacromolecules* **2007**, *8*, 1359−1384.
(5) Lenoir, S.; Pagnoulle, C.; Galleni, M.; Compere, P.; Jérôme, R.; Detrembleur, C. *Biomacromolecules* **2006**, *7*, 2291−2296.
(6) Page, K.; Wilson, M.; Parkin, I. P. *J. Mater. Chem.* **2009**, *19*, 3819−3831.
(7) Lu, L.; Rininsland, F. H.; Wittenburg, S. K.; Achyuthan, K. E.; McBranch, D. W.; Whitten, D. G. *Langmuir* **2005**, *21*, 10154−10159.
(8) Tang, Y. L.; Corbitt, T. S.; Parthasarathy, A.; Zhou, Z. J.; Schanze, K. S.; Whitten, D. G. *Langmuir* **2011**, *27*, 4956−4962.
(9) Zhou, Z. J.; Corbitt, T. S.; Parthasarathy, A.; Tang, Y. L.; Ista, L. F.; Schanze, K. S.; Whitten, D. G. *J. Phys. Chem. Lett.* **2010**, *1*, 3207−3212.
(10) Wang, Y.; Canady, T. D.; Zhou, Z. J.; Tang, Y. L.; Price, D. N.; Bear, D. G.; Chi, E. Y.; Schanze, K. S.; Whitten, D. G. *ACS Appl. Mater. Interfaces* **2011**, *3*, 2209−2214.
(11) Liu, Y.; Ogawa, K.; Schanze, K. S. *Anal. Chem.* **2008**, *80*, 150−158.
(12) Tang, Y.; Achyuthan, K. E.; Whitten, D. G. *Langmuir* **2010**, *26*, 6832−6837.
(13) Our preliminary results from ongoing work show that the CPE and OPE compounds show no toxicity against skin tissue and low toxicity against endothelial and epithelial cells at the concentration where they can efficiently kill bacteria.
(14) Wang, Y.; Tang, Y. L.; Zhou, Z. J.; Ji, E.; Lopez, G. P.; Chi, E. Y.; Schanze, K. S.; Whitten, D. G. *Langmuir* **2010**, *26*, 12509−12514.
(15) Yang, L. H.; Gordon, V. D.; Mishra, A.; Sorn, A.; Purdy, K. R.; Davis, M. A.; Tew, G. N.; Wong, G. C. L. *J. Am. Chem. Soc.* **2007**, *129*, 12141−12147.
(16) Mowery, B. P.; Lee, S. E.; Kissounko, D. A.; Epand, R. F.; Epand, R. M.; Weisblum, B.; Stahl, S. S.; Gellman, S. H. *J. Am. Chem. Soc.* **2007**, *129*, 15474−15476.
(17) Palermo, E. F.; Sovadinova, I.; Kuroda, K. *Biomacromolecules* **2009**, *10*, 3098−3107.
(18) Melo, L. D.; Mamizuka, E. M.; Carmona-Ribeiro, A. M. *Langmuir* **2010**, *26*, 12300−12306.
(19) Wang, Y.; Zhou, Z. J.; Tang, Y. L.; Zhu, J. S.; Canady, T. D.; Chi, E. Y.; Schanze, K. S.; Whitten, D. G. *Polymers* **2011**, *3*, 1199−1214.
(20) Palermo, E. F.; Kuroda, K. *Appl. Microbiol. Biotechnol.* **2010**, *87*, 1605−1615.
(21) Ji, E.; Corbitt, T. S.; Parthasarathy, A.; Schanze, K. S.; Whitten, D. G. *ACS Appl. Mater. Interfaces* **2011**, *3*, 2820−2829.
(22) Graham, J. M.; Higgins, J. A. *Membrane Analysis*; Springer: New York, 1997.
(23) Franklin, T. J.; Snow, G. A. *Biochemistry and Molecular Biology of Antimicrobial Drug Action*, 6th ed.; Springer: New York, 2005.
(24) McDonnell, G.; Russell, A. D. *Clin. Microbiol. Rev.* **1999**, *12*, 147−179.
(25) Timofeeva, L.; Kleshcheva, N. *Appl. Microbiol. Biotechnol.* **2011**, *89*, 475−492.
(26) Zhao, X. Y.; Pinto, M. R.; Hardison, L. M.; Mwaura, J.; Muller, J.; Jiang, H.; Witker, D.; Kleiman, V. D.; Reynolds, J. R.; Schanze, K. S. *Macromolecules* **2006**, *39*, 6355−6366.
(27) Tang, Y. L.; Hill, E. H.; Zhou, Z. J.; Evans, D. G.; Schanze, K. S.; Whitten, D. G. *Langmuir* **2011**, *27*, 4945−4955.
(28) Phospholipid abbreviations: 1,2-dimyristoyl-*sn*-glycero-3-phosphoethanolamine-*N*-(lissamine rhodamine B sulfonyl) (ammonium salt) = DMPE-Rh; 1,2-distearoyl-*sn*-glycero-3-phosphoethanolamine-*N*-(biotinyl(poly(ethylene glycol))-2000) (ammonium salt) = Biotin-PEG-DSPE; 1,2-dioleoyl-*sn*-glycero-3-phosphoethanolamine = DOPE; 1,2-dioleoyl-*sn*-glycero-3-[phospho-*rac*-(1-glycerol)] (sodium salt) = DOPG.
(29) SYTO 60 and SYTOX Green are high-affinity nucleic acid stains. SYTO 60 with red fluorescence is used to stain both live and dead cells. SYTOX Green with green fluorescence is permeable only to compromised cell membranes and is used to indicate cell death.
(30) Corbitt, T. S.; Ding, L. P.; Ji, E. Y.; Ista, L. K.; Ogawa, K.; Lopez, G. P.; Schanze, K. S.; Whitten, D. G. *Photochem. Photobiol. Sci.* **2009**, *8*, 998−1005.
(31) Tanaka, T.; Tamba, Y.; Masum, S. M.; Yamashita, Y.; Yamazaki, M. *Biochim. Biophys. Acta* **2002**, *1564*, 173−182.
(32) Bolinger, P. Y.; Stamou, D.; Vogel, H. *J. Am. Chem. Soc.* **2004**, *126*, 8594−8595.
(33) Mishra, A.; Gordon, V. D.; Yang, L. H.; Coridan, R.; Wong, G. C. L. *Angew. Chem., Int. Ed.* **2008**, *47*, 2986−2989.
(34) Mũnoz-Bonilla, A.; Fernández-García, M. *Prog. Polym. Sci.* **2011**, doi: 10.1016/j.progpolymsci.2011.08.005.
(35) Epand, R. M.; Epand, R. F. *Biochim. Biophys. Acta, Biomembr.* **2009**, *1788*, 289−294.
(36) Wu, M. H.; Maier, E.; Benz, R.; Hancock, R. E. W. *Biochemistry* **1999**, *38*, 7235−7242.
(37) Shai, Y. Mechanism of Membrane Permeation and Pore Formation by Antimicrobial Peptides. In *Protein-Lipid Interactions: From Membrane Domains to Cellular Networks*; Tamm, L. K., Ed.; Wiley-VCH: Weinheim, Germany, 2005.
(38) Wang, Y.; Chi, E. Y.; Schanze, K. S.; Whitten, D. G. Unpublished work.
(39) Koltover, I.; Salditt, T.; Radler, J. O.; Safinya, C. R. *Science* **1998**, *281*, 78−81.
(40) Yang, L. H.; Gordon, V. D.; Trinkle, D. R.; Schmidt, N. W.; Davis, M. A.; DeVries, C.; Som, A.; Cronan, J. E.; Tew, G. N.; Wong, G. C. L. *Proc. Natl. Acad. Sci. U.S.A.* **2008**, *105*, 20595−20600.
(41) Seddon, J. M.; Robins, J.; Gulik-Krzywicki, T.; Delacroix, H. *Phys. Chem. Chem. Phys.* **2000**, *2*, 4485−4493.
(42) Wimley, W. C. *ACS Chem. Biol.* **2010**, *5*, 905−917.